Journal of Non-Newtonian Fluid Mechanics, 11 (1982) 175–199
Elsevier Scientific Publishing Company, Amsterdam—Printed in The Netherlands

NON-ISOTHERMAL FLOW OF A MOLTEN POLYMER IN A NARROW RECTANGULAR CAVITY

H VAN WIJNGAARDEN, J F DIJKSMAN
Philips' Research Laboratories, Eindhoven (The Netherlands)
and
P WESSELING
Delft University of Technology, Delft (The Netherlands)

(Received January 4, 1982, in revised form February 26, 1982)

Summary

An accurate and stable numerical scheme is presented for the calculation of the non-isothermal flow of a non-Newtonian liquid in a narrow rectangular cavity The effects of solidification of matter on the walls of the cavity during filling and viscous heating are taken into account. The viscosity of the liquid model used is shear rate and temperature dependent

List of symbols

A	temperature coefficient
b	temperature coefficient
c_p	heat capacity of fluid
c_{ps}	heat capacity of solidified layer
H	heat transfer coefficient
$2h$	height of channel
k	thermal conductivity of fluid
k_s	thermal conductivity of solidified layer
l	length of cavity
l^*	position of flow front during filling
m_0	coefficient Power-law model
n	Power-law index
n	normal to the moving boundary

0377-0257/82/0000–0000/$02 75

p	pressure
p_{max}	maximum attainable pressure at entrance
Q^*	volume flux through gate
t	time
t_c	contact time
T	temperature in fluid
T_s	temperature in solidified layer
T_o	coolant temperature
T_m	transition temperature
T_b	injection temperature
T_w	wall temperature
T_{core}	temperature of core
u_1, u_2	velocity components in the x_1- and x_2-directions, respectively
V	mean injection velocity
v_n	normal velocity of moving boundary
$\tilde{v}_2$	velocity component of moving boundary in the x_2-direction
w	width of channel
x_1, x_2	coordinates, x_1 flow direction, x_2 transverse direction
δ	x_2-coordinate of moving boundary
λ	latent heat of fusion
η	viscosity
ρ	density of fluid
ρ_s	density of solidified layer

Dimensionless symbols

Q	flux $= Q^* / 2Vh$
s	coordinate along streamline
u	velocity component x-direction $= u_1 / V$
v	velocity component y-direction $= u_2 / \epsilon V$
$\tilde{v}$	velocity component of moving boundary in the y-direction
x	coordinate stream direction $= x_1 / L$
y	coordinate height direction $= x_2 / h$
x_k	x-coordinate grid line
y_k^l	y-coordinate intersection of grid line x_k with streamline l
α_i	y-coordinate of moving boundary during iteration
α	y-coordinate of moving boundary $= \delta / h$
β	number needed to define the grid
γ	shear rate
Δs	step size along streamline
Δx	step size in x-direction
ϵ	small parameter ($\epsilon = h/l$)
π	pressure $= \epsilon p / \rho V^2$

π_0 ambient pressure
π_{max} maximum pressure
τ time $= \epsilon Vt/h$
$\hat{\tau}$ time at which moving boundary passes grid point
θ temperature $= (T - T_b)/(T_m - T_o)$
θ_k^l temperature at intersection of grid line x_k and streamline l
θ^* interpolated temperature for previous time step

Dimensionless numbers
$Re = \rho h V/\eta_0$
$Gz = \epsilon Pe = \epsilon \rho c_p Vh/k$
$Gz_s = \epsilon \rho_s c_{ps} Vh/k_s$
$Br = \eta_0 V^2/\{k(T_m - T_o)\}$
$Na = b\eta_0 V^2/(kA)$
$Bi = Hh/k_s$
$Ste = c_p(T_m - T_o)/\lambda = Ac_p/(b\lambda)$
with $\eta_0 = m_0(V/h)^{n-1}$

1. Introduction

Injection moulding is an industrial process for the manufacture of thin-walled or small thermoplastic products During the process the raw material is first heated up to a temperature at which it becomes easily deformable The material is then injected into the mould Thermoplastics are poor heat conductors To keep the cooling time short enough, even for thin-walled products, to allow the mould to be re-used at a sufficiently high rate, the mould walls must be kept at a temperature far below the melting or glass transition temperature

In this paper an analysis is given of the flow behaviour of a molten polymer which is injected into a rectangular cavity at a fairly high speed An example of such a cavity is shown in Fig 1

The cavity was used by Wales, Van Leeuwen and Van der Vijgh [1] to investigate experimentally the orientation distribution in the product for several process conditions In their experiments the cavity is filled at a constant rate and the filling stage is terminated as soon as the flow front has reached the end of the mould Among other things, they determined the

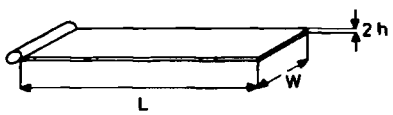

Fig 1 Rectangular cavity

pressure distribution along the axis of the mould at several instants during the filling stage and the orientation distribution at several axial positions

Janeschitz-Kriegl [2,3] and Dietz et al [4,5] tried to explain the experimental results obtained by Wales et al by means of approximate calculations concerning the flow and temperature field

In our analysis we shall leave out of account the influence of the width of the channel The flow can therefore be considered to be two-dimensional, provided that w is much larger than $2h$

The flow in the cavity can be characterized by a set of dimensionless numbers, such as Re, $Pé$, Br, Bi and Ste The Reynolds number Re relates inertia forces to viscous forces The Péclet number $Pé$ is defined as the ratio of the heat convected in the flow direction and the heat transported to the walls by conduction The Brinkman number Br gives a measure of the extent to which viscous heating is important in view of the heat flow towards the walls by conduction The Biot number Bi tells something about the capability of the walls of the cavity to transport heat to the cooling liquid Finally, the Stefan number Ste relates the heat capacity of the material considered to the transition heat needed to overcome a change in state of aggregation [6–8]

In the processing of polymers the Reynolds number Re is typically very small, the Péclet number $Pé$ is very large and the Brinkman number Br ranges from unity to a moderately high value When the mould is cooled properly the Biot number Bi is large The Stefan number Ste is high

As the Reynolds number Re is low, disturbances of the fully developed flow profile are rapidly damped [6] In the case where there are no rapid changes in the flow field we may expect that a fully developed flow will exist at any instant and at any place A high Peclet number Pe means that temperature gradients along the streamlines are small compared with those normal to them Moreover, disturbances of the temperature field are noticeable over quite long time intervals

From the data presented by Wales et al [1] it appears that the Brinkman number of their experiments is of order unity (There is a misprint in the paper by Janeschitz-Kriegl [2] Instead of $Br = 0\ 145$ one should read $Br = 3\ 52$)

For the case where the Brinkman number is very small and the viscosity depends only on temperature, a theoretical basis for the study of this type of flow has been given by Ockendon and Ockendon [9] They considered the flow of a fluid of uniform temperature entering a channel, the walls of which are kept at a low temperature Due to the cooling action a layer of relatively low temperature grows with increasing distance from the entrance Since the viscosity increases with decreasing temperature, the fluid is forced in the beginning of the channel to follow the hot regions The velocity in these hot

jet regions is higher than in the upstream Poiseuille flow Far downstream the liquid has completely reached the wall temperature and flows again according to Poiseuille

For very high Brinkman numbers Pearson [7] and Ockendon [8] have shown that in the beginning of the channel close to the walls there is a very significant temperature rise This is because the frictional heat, generated in the high shear rate regions close to the walls, cannot be transported quickly enough to the walls and to the interior of the fluid domain Downstream at a higher temperature an equilibrium will be reached between the frictional heat and the heat flow towards the walls by conduction

Our aim is to present a stable and accurate numerical scheme with which to solve the equations governing the fluid flow and temperature distribution during the filling process inside the cavity at moderately high Brinkman numbers For most practical purposes the Brinkman number lies between unity and a moderately high value

Because of the existence of solidified layers on the walls the flow domain will no longer be a rectangle A dimensional analysis shows that the one-dimensional description of the non-isothermal flow of a polymer melt in this configuration is not correct [7] The transport of heat by convection in the direction normal to the walls cannot be left out of account In the neighbourhood of the moving boundary this type of heat flow will dominate the heat transport by convection in the flow direction This is due to the fact that, although the normal velocity in that region is very small, the temperature gradient in the normal direction is very large This effect increases with increasing Brinkman number

2. Mathematical model

As mentioned earlier, we confine ourselves to the analysis of a two-dimensional flow of a molten polymer Since there is immediate solidification on the walls during filling, the domain of calculation must be divided into two parts, i e a fluid domain and a solid domain which are separated by an interface, called the moving boundary (Fig 2)

From the description of the process it may be clear that injection moulding is highly unsteady In most cases, however, the flux through the entrance of the cavity is constant up to the moment that the maximum pressure of the pump is reached After that instant the pressure is kept constant at its maximum value and the flux decreases rapidly (Fig 3)

During the constant flux period we consider a short section of the channel after the flow front has passed For this section it does not matter what actually happens at the flow front The flow in such a region may therefore be expected to be rather stationary It is not even important that the

maximum pressure is reached after a while or what the magnitude of this pressure is Formally we can choose this pressure so high that we can always take the observation time long enough to have a low Deborah number, which

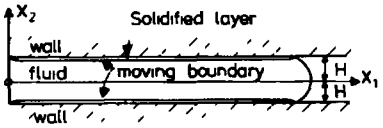

Fig 2 Domain of interest

is defined as the ratio between the relaxation time of the fluid and the observation time The approximate behaviour of the molten polymer during the constant flux period is therefore essentially fluid-like

We assume that this statement is correct for the constant pressure period too The constitutive equation chosen is the generalized Newtonian model The logarithm of the viscosity η depends linearly on the logarithm of the shear rate γ The temperature dependence is entered by an exponential type of expression Hence

$$\eta = m_0 \exp(-A(T - T_b)/(T_m - T_0))\, \gamma^{n-1} \tag{2 1}$$

We assume that m_0, A, n, c_p, c_{ps}, k, k_s, λ, ρ and ρ_s are constants

The equations governing the problem, namely the continuity equation, the equations of motion and the energy equations in the fluid and solid domain respectively are (summation convention is used)

$$\frac{\partial u_i}{\partial x_i} = 0, \tag{2 2a}$$

$$\rho\left(\frac{\partial u_i}{\partial t} + u_j \frac{\partial u_i}{\partial x_j}\right) = -\frac{\partial P}{\partial x_i} + \frac{\partial}{\partial x_j}\eta\left(\frac{\partial u_i}{\partial x_j} + \frac{\partial u_j}{\partial x_i}\right). \tag{2 2b}$$

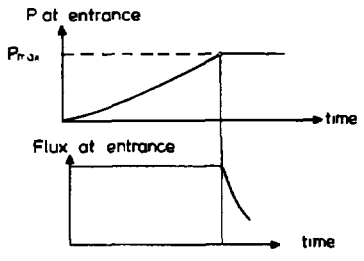

Fig 3 Pressure and flux at the entrance as functions of time

$$\rho c_p\left(\frac{\partial T}{\partial t}+u_j\frac{\partial T}{\partial x_j}\right)=k\frac{\partial^2 T}{\partial x_j\partial x_j}+\eta\gamma^2, \tag{2 2c}$$

$$\rho_s c_{ps}\frac{\partial T}{\partial t}=k_s\frac{\partial^2 T}{\partial x_j\partial x_j}, \tag{2 2d}$$

$$\gamma=\sqrt{\frac{1}{2}\left(\frac{\partial u_i}{\partial x_j}+\frac{\partial u_j}{\partial x_i}\right)\left(\frac{\partial u_i}{\partial x_j}+\frac{\partial u_j}{\partial x_i}\right)} \tag{2 2e}$$

(Bird, Armstrong and Hassager [10])

These equations are subjected to the following boundary conditions
At the flow front $x_1 = l^*$, only the pressure is prescribed, which is arbitrarily defined to be zero (ambient pressure)

$$p(l^*, x_2)=0 \tag{2 3a}$$

We assume that the problem is symmetric with respect to the line $x_2 = 0$, hence

$$\frac{\partial T}{\partial x_2}(x_1, 0)=\frac{\partial u_1}{\partial x_2}(x_1, 0)=u_2(x_1, 0)=0 \tag{2 3b}$$

At the entrance $x_1 = 0$ we prescribe the temperature and either the volume flux or the pressure

$$T(0, x_2)=0,$$

$$\text{if } p(0, x_2)<p_{\max} \text{ then } \int_{-h}^{+h} u_1(0, x_2)\,dx_2=Q^*$$

otherwise

$$p(0, x_2)=p_{\max} \tag{2 3c}$$

At $x_2 = h$, i e at the wall of the cavity, the transport of heat depends on the temperature gradient that can be maintained in the wall by the coolant Assuming that this gradient is constant we have

$$k_s\frac{\partial T_s}{\partial x_2}(x_1, h)+H(T_w-T_0)=0, \tag{2 3d}$$

domain and H the heat transfer coefficient [11] In most cases H is very large, so $T_w \approx T_0$

The velocity of the moving boundary depends on the temperature gradi-

ents in the liquid and solid phase at the moving boundary

$$\lambda \rho v_n = k_s \frac{\partial T_s}{\partial n} - k \frac{\partial T}{\partial n}, \tag{2.4}$$

where $\partial/\partial n$ means differentiation in the direction of the normal to the moving boundary, which is positive towards the wall, and v_n is the velocity in the direction of the normal [12] To obtain the boundary conditions along the moving boundary we use conservation of mass for a small portion of the domain with length Δx_1 after the flow front has passed

During a time increment Δt the moving boundary is displaced through a distance $v_n \Delta t$ in the direction of the normal Due to the difference in specific mass between the solid and the liquid phases the total mass M in the domain with length Δx_1 changes as follows

$$\mathrm{d}M/\mathrm{d}t = (\rho - \rho_s)\, \Delta x_1\, \partial\delta/\partial t \tag{2.5}$$

The position of the moving boundary is given by $x_2 = \delta(x_1, t)$ Conservation of mass requires

$$\frac{\mathrm{d}M}{\mathrm{d}t} = \rho \int_0^{\delta} u_1\, \mathrm{d}x_2 \Big|_{x_1}^{x_1 + \Delta x_1} \tag{2.6}$$

Combining (2.5) and (2.6) and letting $\Delta x_1 \to 0$ results in

$$(\rho - \rho_s)\, \partial\delta/\partial t = -\rho u_1(x_1, \delta)\, \partial\delta/\partial x_1 + \rho u_2(x_1, \delta), \tag{2.7}$$

where we have used the continuity equation $\partial u_1/\partial x_1 + \partial u_2/\partial x_2 = 0$ The no-slip condition along the moving boundary reads

$$u_1(x_1, \delta) + u_2(x_1, \delta)\, \partial\delta/\partial x_1 = 0 \tag{2.8}$$

Solving (2.7) and (2.8) for $u_1(x_1, \delta)$ and $u_2(x_1, \delta)$ we find

$$u_1(x_1, \delta) = -\left(1 - \frac{\rho_s}{\rho}\right) \frac{\partial\delta/\partial x_1}{1 + (\partial\delta/\partial x_1)^2} \frac{\partial\delta}{\partial t}, \tag{2.9}$$

$$u_2(x_1, \delta) = \left(1 - \frac{\rho_s}{\rho}\right) \frac{1}{1 + (\partial\delta/\partial x_1)^2} \frac{\partial\delta}{\partial t}$$

In the following we assume that $\rho_s = \rho$, so considering the fact that the temperature of the moving boundary equals the transition temperature, we may write

$$u_1(x_1, \delta) = u_2(x_1, \delta) = 0 \qquad T(x_1, \delta) = T_m \tag{2.10}$$

The equations are put into dimensionless form by introducing the following dimensionless variables

$$\tau = (\epsilon V/h)t, \quad x = x_1/l = \epsilon x_1/h, \quad y = x_2/h,$$

$$u = u_1/V, \quad v = u_2/\epsilon V, \quad Q = Q^*/(2Vh),$$

$$\pi = \epsilon p/\rho V^2, \quad \theta = (T - T_b)/(T_m - T_0), \tag{2 11}$$

where $\epsilon = h/l$ and V is the mean velocity at the entrance

We now assume that $\epsilon \ll 1$, i e the channel is assumed to be long and narrow This assumption is exploited by constructing the following asymptotic channel approximation We develop u, v, π and θ in power series in ϵ, and keep only the leading terms as $\epsilon \to 0$ We obtain

$$\partial u/\partial x + \partial v/\partial y = 0,$$

$$\frac{\partial \pi}{\partial x} = Re^{-1} \frac{\partial}{\partial y} \mathrm{e}^{-A\theta} \left| \frac{\partial u}{\partial y} \right|^{n-1} \frac{\partial u}{\partial y},$$

$$\partial \pi/\partial y = 0,$$

$$\frac{\partial \theta}{\partial \tau} + u\frac{\partial \theta}{\partial x} + v\frac{\partial \theta}{\partial y} = \frac{1}{Gz} \frac{\partial^2 \theta}{\partial y^2} + \frac{Br}{Gz} \mathrm{e}^{-A\theta} \left| \frac{\partial u}{\partial y} \right|^{n+1},$$

$$\frac{\partial \theta_\infty}{\partial \tau} = \frac{1}{Gz_\infty} \frac{\partial^2 \theta_\infty}{\partial y^2}, \tag{2 12}$$

which set can be considered as a consistent first-order approximation of the original equations

The Reynolds, Graetz and Brinkman numbers are defined by

$$Re = \rho h V/\eta_0, \quad Gz = \epsilon \rho c_p V h/k,$$

$$Br = \eta_0 V^2/\{k(T_m - T_0)\}, \tag{2 13}$$

where

$$\eta_0 = m_0 (V/h)^{n-1}$$

In fact the number relating the inertia forces to the viscous forces is equal to ϵRe After substituting $b = A/(T_m - T_0)$ the Brinkman number becomes the Nahme–Griffith number Na [6–8]

$$Na = b\eta_0 V^2/(kA) \tag{2 14}$$

The boundary conditions in dimensionless form are

$$\pi(l^*/l, y) = \pi_0, \tag{2 15a}$$

$$v(x, 0) = \frac{\partial u}{\partial y}(x, 0) = \frac{\partial \theta}{\partial y}(x, 0) = 0, \tag{2 15b}$$

if $\pi(0, y) < \pi_{max}$ then $\int_0^1 u(0, y)\,dy = 1$ otherwise $\pi(0, y) = \pi_{max}$.

$$\theta(0, y) = 0, \tag{2 15c}$$

$$u(x, \alpha) = v(x, \alpha) = 0, \quad \theta(x, \alpha) = \theta_m, \tag{2 15d}$$

$$\frac{\partial \theta_s}{\partial y}(x, 1) + Bi\{\theta_s(x, 1) - \theta_0\} = 0, \tag{2 15e}$$

where the Biot number Bi is defined by

$$Bi = Hh/k_s \tag{2 16}$$

The dimensionless channel approximation to (2 4), which governs the velocity of the moving boundary, is obtained as follows Equation (2 4) can be rewritten as

$$\lambda \rho v_n = (1 + \delta'^2)^{-1/2}(-\delta' \partial/\partial x_1 + \partial/\partial x_2)(k_s T_s - kT)|_{x_2 = \delta}, \tag{2 17}$$

where $\delta' = \partial\delta/\partial x_1$ The dimensionless form of (2 17) is found to be

$$\frac{v_n}{V} = \epsilon \frac{Ste}{Gz}(1 + \epsilon^2 \alpha'^2)^{-1/2}\left(-\epsilon^2 \alpha' \frac{\partial}{\partial x} + \frac{\partial}{\partial y}\right)\left(\frac{k_s}{k}\theta_s - \theta\right)|_{y=\alpha}, \tag{2 18}$$

where $\alpha' = \partial\alpha/\partial x$ and the Stefan number Ste is given by

$$Ste = (T_m - T_0)c_p/\lambda = Ac_p/(b\lambda) \tag{2 19}$$

The components of v_n are $(1 + \epsilon^2 \alpha'^2)^{-1/2} v_n(-\epsilon\alpha', 1)$ Hence, to leading order, $v_n \approx \tilde{v}_2$ From (2 18) we conclude that $v_n = O(\epsilon)$ which is consistent with the channel approximation Accordingly, we put $\tilde{v}_2 = \epsilon V \tilde{v}$ In this way, the first approximation of (2 18) is found to be

$$\tilde{v} = \frac{Ste}{Gz}\frac{\partial}{\partial y}\left(\frac{k_s}{k}\theta_s - \theta\right)|_{y=\alpha} \tag{2 20}$$

Integration of the equation of motion in the y-direction yields, under the assumption that $\partial\pi/\partial x < 0$,

$$\frac{\partial \pi}{\partial x}(x, \tau) = \frac{Q^n}{Re}\left\{\int_0^\alpha e^{A\theta^n} y^{1+1/n}\,dy\right\}^{-n}, \tag{2 21a}$$

$$u = Q\int_y^\alpha e^{A\theta^n} y^{1/n}\,dy \Big/ \int_0^\alpha e^{A\theta^n} y^{1+1/n}\,dy \tag{2 21b}$$

As soon as the temperature field θ is known the pressure drop $\partial\pi/\partial x$ and the velocity u can be found by evaluation of the expressions (2 21a) and (2 21b)

3. Numerical approximation

Suppose we have calculated the flow for $\tau = \tau_j$ ($j = 1, 2, \ldots, i-1$) and for $\tau = \tau_i$ the position of the moving boundary We define our grid at $\tau = \tau_i$ as follows Let the grid lines $x = x_k$ for $k = 0, 1, \ldots, i-1$ be the same as the grid lines at $\tau = \tau_{i-1}$, and let the grid line $x = x_i$ be the front line of the flow When the flux Q is known the position of this line can be calculated

$$x_i - x_{i-1} = \int_{\tau_{i-1}}^{\tau} Q(\tau)\, d\tau \tag{3 1}$$

Define on the line $x = x_0$ (beginning of the channel) the grid points $y = y_0^l$, $l = 0, 1, \ldots, L$, where y_0^0 lies on the symmetry line of the channel and y_0^L on the wall The intersections of the instantaneous streamlines through those points and the grid lines $x = x_k$ are the grid points in our liquid domain One advantage of this definition is that the position of the moving boundary is defined by the grid points y_k^L, as this boundary is a streamline Another advantage is that the convection term in the energy equation can be expressed in a simple way

$$u\partial\theta/\partial x + v\partial\theta/\partial y = u_s\partial\theta/\partial s, \tag{3 2}$$

where s measures the distance along the streamline

The main problem is now the calculation of the position of the grid points This calculation is based on the idea that the flux through two adjacent grid points on $x = x_0$ and two corresponding adjacent grid points on any other grid line must be equal Suppose that we know the position of the grid points, the velocity and temperature on some grid line $x = x_{k-1}$ The first step of the iterative method is that we choose $L + 1$ grid points on $x = x_k$, where y_k^0 lies on the symmetry line, y_k^L on the moving boundary, and $y_k^{l-1} < y_k^l$ After we have approximated the temperature at these grid points with a finite difference scheme, we are able to calculate the velocity u with the Simpson rule from (2 21b) Now we rearrange the grid points in such a way that the flux through two adjacent grid points equals the flux through the two corresponding points on $x = x_0$ This process must be repeated if the position of the grid points is not accurate enough If we choose, as a first guess, the grid points on $x = x_k$ such that the ratio of the distances between points on x_k and the corresponding points on x_{k-1} is equal to the ratio between the corresponding positions of the moving boundary y_k^l and y_{k-1}^l, then one iteration step usually suffices to obtain an accurate approximation of the position of the grid points

We will now consider the finite difference scheme for the temperature At a point (x_k, y_k^l) the convective term (3 2) can be approximated by (see Fig 4)

$$u_s \frac{\partial\theta}{\partial s} \approx u_{s_{k-1}}^l \frac{\theta_k^l - \theta_{k-1}^l}{\Delta s} \tag{3 3}$$

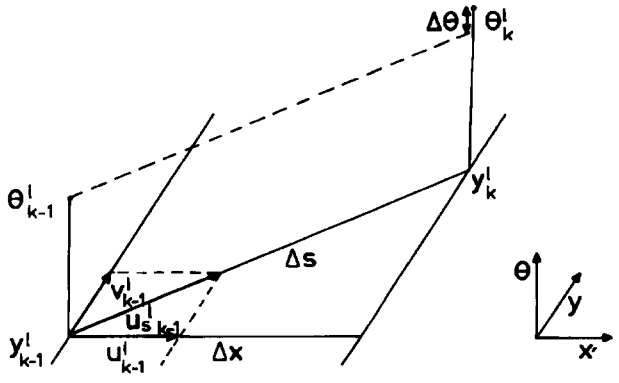

Fig 4 Definition of Δx, Δy and Δs (Eqn 3 4)

Unless stated otherwise, $\tau = \tau_1$, the current time level Hence (3 3) is an implicit approximation Now we have

$$\frac{u^l_{s_{k-1}}}{\Delta s} = \frac{u^l_{k-1}}{\Delta x} \tag{3 4}$$

Hence

$$u_s \frac{\partial \theta}{\partial s} \approx u^l_{k-1} \frac{\theta^l_k - \theta^l_{k-1}}{\Delta x} \tag{3 5}$$

For the approximation of the non-stationary term in the energy equation we have to know the value of $\theta = \theta^*$ at $\tau = \tau_{l-1}$ (previous moment) at the points (x_k, y^l_k) As the positions of the grid points are time-dependent, this value has to be interpolated, e g linearly The conduction is approximated implicitly (central differences) and the viscous heating term explicitly This results in the following scheme

$$\frac{\theta^l_k - \theta^*}{\Delta\tau} + u^l_{k-1} \frac{\theta^l_k - \theta^l_{k-1}}{\Delta x}$$

$$= \frac{2}{Gz\, \Delta^l_k y\, \Delta^{l+1}_k y} \left(\frac{\Delta^l_k y}{\Delta^{l+1}_k y + \Delta^l_k y} \theta^{l+1}_k - \theta^l_k + \frac{\Delta^{l+1}_k y}{\Delta^{l+1}_k y + \Delta^l_k y} \theta^{l-1}_k \right)$$

$$+ \frac{Br}{Gz} \exp\left(\frac{A}{n} \theta^* \right) \left(-Re \frac{\partial \pi^*}{\partial x} y^l_k \right)^{1+1/n}, \tag{3 6}$$

where $\Delta^l_k y = y^l_k - y^{l-1}_k$, and the symbol * denotes the interpolated value for $\tau = \tau_{l-1}$ at the point (x_k, y^l_k)

Together with the boundary conditions, this scheme leads to a tri-diagonal matrix equation In our liquid domain we have to carry out a set of iterations in order to find the grid points on each line x_k, which can be treated one by

one, starting at the entrance In the solidified layer we have to solve the parabolic energy equation on any grid line This can be done with an implicit central difference scheme The distances between the grid points on the same grid line are equal A problem can arise, however Because of the increasing thickness of the solidified layer it may happen that a grid point is in the solidified layer at $\tau = \tau_i$, but was in the liquid domain at $\tau = \tau_{i-1}$ Then $\partial\theta/\partial\tau$ has to be approximated by

$$\partial\theta/\partial\tau \approx (\theta_k^l - \theta_m)/(\tau_i - \hat{\tau}), \tag{3 7}$$

with $\hat{\tau}$ the time at which the moving boundary passes y_k^l Assuming that we know the position of the moving boundary on x_k for $\tau = \tau_i$ and $\tau = \tau_{i-1}$, $\hat{\tau}$ can be found by interpolation

For the calculation of the solution at $x = x_k$ one problem remains, i e the determination of the position of the moving boundary $\alpha(\tau_i, x_k)$ For this purpose equation (2 20) is used With the solution at the grid lines $x = x_k$, $k = 1, 2, \ldots, i-1$, the right-hand side of (2 20) can be evaluated according to the numerical scheme just outlined, if $\alpha(\tau_i, x_k)$ is given Hence, this right-hand side is a function of α only, and is denoted by $g(\alpha(\tau_i, x_k))$ Therefore (2 20) can be rewritten as follows

$$\partial\alpha(\tau, x_k)/\partial\tau = g(\alpha(\tau, x_k)) \tag{3 8}$$

We have found numerically that g varies rapidly with α Therefore we approximate (3 8) by a stiffly stable numerical scheme, namely the implicit Euler method

$$\alpha(\tau_i, x_k) = \alpha(\tau_{i-1}, x_k) + (\tau_i - \tau_{i-1})\, g(\alpha(\tau_i, x_k)) \tag{3 9}$$

This nonlinear equation is solved approximately by the Regula Falsi method combined with Aitken acceleration Let α_j, $j = 0, 1, 2, \ldots$ be successive approximations to $\alpha(\tau_i, x_k)$ The algorithm is defined as follows

$\alpha_0 = \alpha(\tau_{i-1}, x_k)$,

$\alpha_1 = \frac{3}{2}\alpha_0 - \frac{1}{2}\alpha(\tau_{i-2}, x_k)$,

Regula Falsi

$for\ j = 2, 3\ do\ \alpha_j = \{\alpha_0 g(\alpha_{j-1}) - \alpha_{j-1} g(\alpha_0)\}/\{g(\alpha_{j-1}) - g(\alpha_0)\}$.

Aitken acceleration

$\alpha_4 = (\alpha_1\alpha_3 - \alpha_2^2)/(\alpha_1 + \alpha_3 - 2\alpha_2)$

The method just described enables us to solve the set of equations numerically if the flux Q is known When the maximum pressure has been reached at the entrance of the channel, the flux has to be adjusted Integra-

tion of equation (2 21a) yields

$$\pi_0 - \pi_{\text{entrance}} = -\frac{Q''}{Re}\int_0^{l^*} l\left\{\int_0^{\alpha(x)} e^{4\theta\, n} y^{1+1\, n}\, dy\right\}^{-n} dx \qquad (3\ 10)$$

It is found that the integral on the right-hand side does not change very much if the variations of Q are not to large This indicates that the time for the adjustment of the temperature distribution is much longer than the time scale for changes in Q So equation (3 10) expresses that the pressure at the entrance is approximately proportional to Q'' Using this result a new Q can be obtained from

$$Q_{\text{new}} = Q_{\text{prev}}\left(\frac{\pi_{\max} - \pi_0}{\pi(Q_{\text{prev}}) - \pi_0}\right)^{1\, n}. \qquad (3\ 11)$$

where $\pi(Q_{\text{prev}})$ is the calculated value of π at the entrance for $Q = Q_{\text{prev}}$ The value of Q can be adjusted at every iteration step during which the moving boundary is calculated

4. Results and discussion

The theory presented in the previous sections has been applied to the filling of the mould (see Fig 1) The dimensions of the mould are $l = 0\ 3$ m, $w = 0\ 075$ m, $h = 0\ 001$ m (these are the same dimensions as used by Wales, Van Leeuwen and Van der Vijgh [1], Janeschitz-Kriegl [3] and Dietz and White [4]) The calculations were carried out for the polystyrene used by the authors just referred to The properties needed for the calculation are listed in Table 1

Unless otherwise stated, the mould is filled in 80 time steps In the x-direction 20 grid points are used, 15 in the fluid domain and 5 in the solidified layer At the entrance the grid points in the y-direction are chosen

TABLE 1

Physical properties of PS 678 DOW (Janeschitz-Kriegl [3] Dietz and White [4], Wales [13] and [14])

η	$=6700 \exp(-0\ 017(T - 220°C))\ \gamma^{0\ 356-1}$ Pa s
k	$=0\ 1295$ J/(s m K) ($k_s = k$)
ρ	$=1060$ kg/m^3
c_p	$=1733$ J/(kg K) ($c_{p_s} = c_p$)
T_m	$=100°C$ (glass transition temperature)
λ	$=3400$ J/kg (transition heat at T_m)

in such a way that

$$y_0^l = (1-\beta^l)/(1-\beta^L), \tag{4 1}$$

where $L = 14$ and the index l ranges from 0 to 14 The parameter β is taken equal to 0 9 in order to obtain a finer mesh in the neighbourhood of the wall In the solidified layer the grid points are equidistant

We first consider the case discussed by Wales et al and Janeschitz-Kriegl The polymer is injected at 250°C through a gate at $x = 0$ into a mould, the walls of which are kept at 50°C The mould is filled in 2 5 s The injection speed V is 0 12 m/s The Reynolds, Graetz, Brinkman, Biot and Stefan numbers for this problem are

$Re = 6\,9 \times 10^{-4}$, $Bi = 7\,7 \times 10^{3}$,
$Gz = 17$, $Ste = 25$,
$Br = Na = 0\,4$,

where $\epsilon = 0\,01$, $\eta_0 = 184$ Pa s, $H = 10^6$ J/(s m^2 K) and $A = 0\,85$ The Reynolds number is very small indeed The Graetz number is not very large, so the influence of conduction is significant when the length scales are equal to the length of the mould The Brinkman number is of order unity, which means that the influence of viscous heating must be noticeable

Figure 5 shows the pressure distribution along the axis of the mould The growth of the solidified layer as a function of time and space is presented in Fig 6 The streamlines, i e lines that separate regions of constant instantaneous volume flux, for the case where the flow front reaches the end of the mould, are displayed in Fig 7 Figure 8 gives the isotherms at that instant

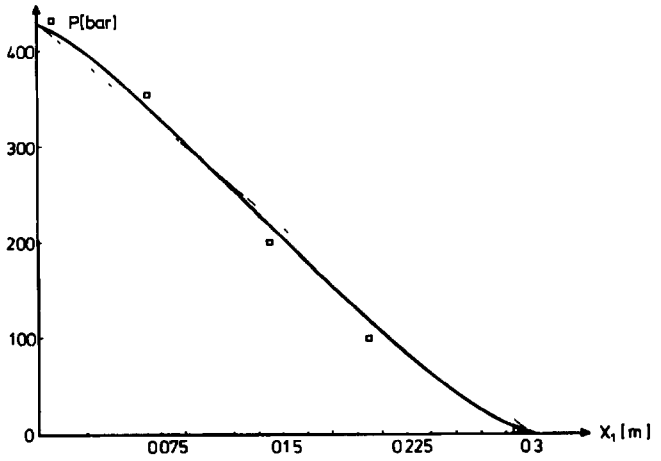

Fig 5 Pressure distribution along the axis of the mould at the end of the filling stage ⊡ Measurements by Wales et al [1]

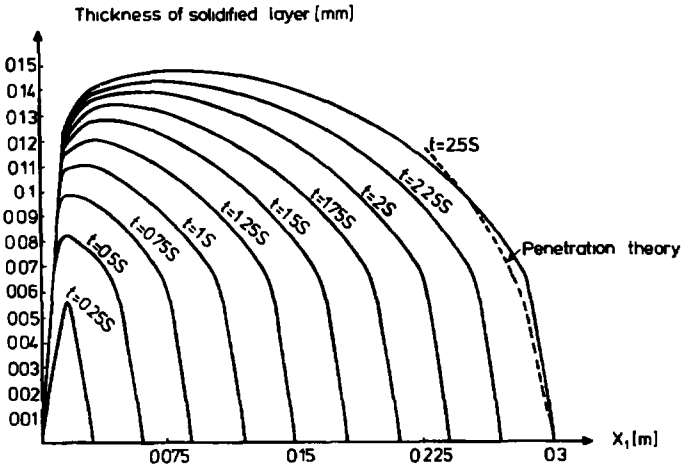

Fig 6 Growth of the solidified layer as a function of time and position The dashed line is an isotherm according to penetration theory

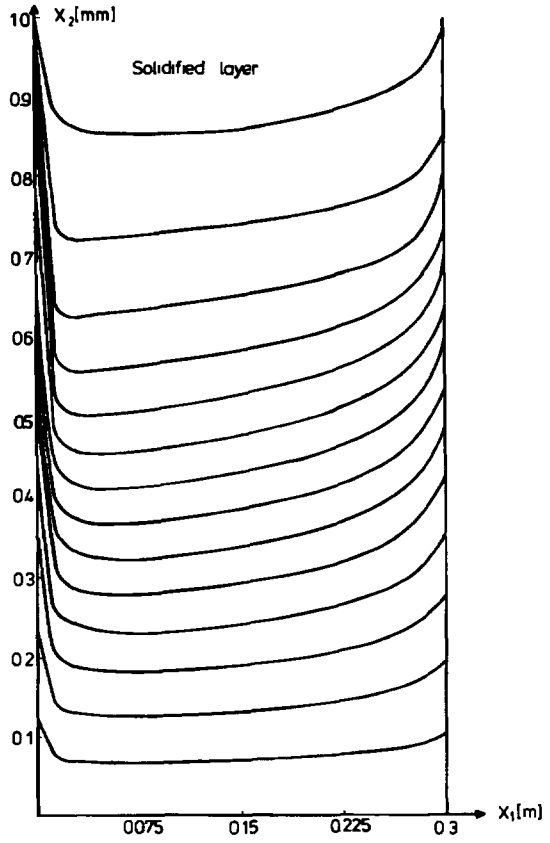

Fig 7 Streamlines for the moment that the mould has just been filled

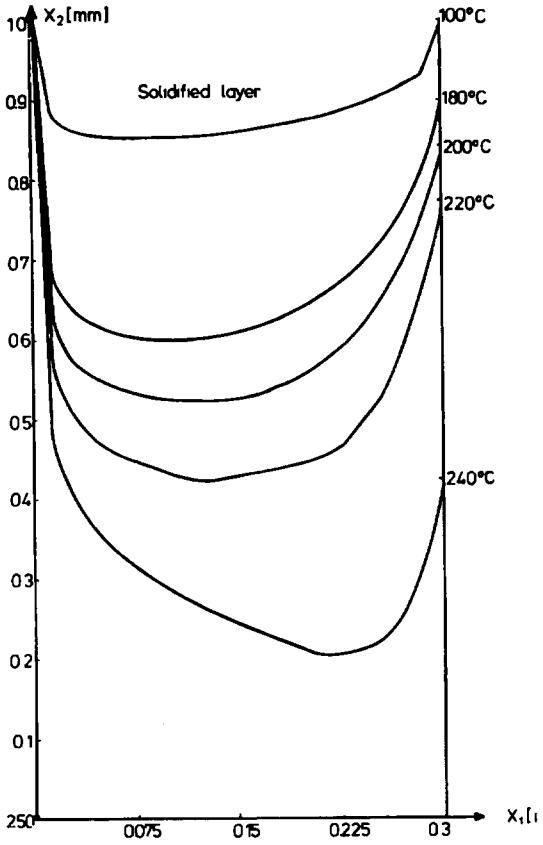

Fig 8 Isotherms for the moment that the mould has just been filled

It should be noted that the results at the very beginning and the end of the flow field are not as accurate as in the remaining part of the domain because there the channel approximation breakes down In the entrance there are large temperature gradients in the x-direction, while at the end of the flow field the flow is essentially two-dimensional [15] Dietz and White [4] and Janeschitz-Kriegl [3] have presented a method to obtain at least an approximate impression of this last-mentioned effect They stated that hot material is transported in the flow front from the core to the walls When this hot material hits the wall it is cooled immediately, roughly according to the penetration theory

$$T - T_w = (T_{\text{core}} - T_w)\ \text{erf}\left\{\frac{(h - x_2)}{2\sqrt{kt_c/\rho c_p}}\right\}. \tag{4 2}$$

where t_c stands for the contact time The moving boundary is given by the isotherm $T = T_m$ This line is shown in Fig 6 for $T_{core} = 244°C$ (When the end of the filling stage is approached the temperature in the core is somewhat lower than the injection temperature) The thickness of the solidified layer found by applying (4 2) is an upper limit We see that according to the present theory the isotherm lies somewhat above the maximum "allowable" layer thickness In our analysis the influence of the "fountain" effect on the temperature distribution is neglected From the results shown it appears that this effect is noticeable over approximately 10% of the length of the mould

As can be seen from Fig 7, the streamlines are more or less uniformly shaped The same applies to the previous time steps This means that except in the entrance region there is a positive velocity component in the y-direction Consequently there is convective transport of heat from the relatively hot core to the regions closer to the walls The heat generated by internal friction increases with increasing distance from the entrance At the end of the filling stage these two contributions become more important than the heat removed by conduction in the y-direction This explains qualitatively the temperature rise at the end of the mould when the filling stage terminates The pressure profile has the typical S-shape experimentally observed by Wales et al [1]

We made a comparison between our findings on the solidified layer thickness distribution along the walls of the mould at the moment the mould is just filled and those predicted by the theories of Dietz and White [4] and

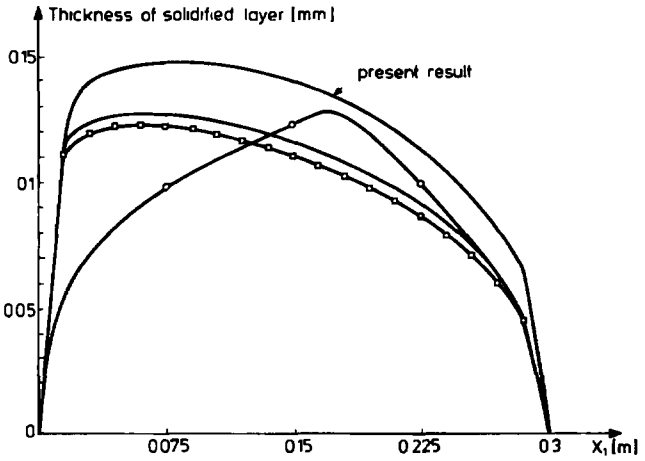

Fig 9 Thickness of the solidified layer as a function of x_f according to the theories of Dietz and White [4] and Janeschitz-Kriegl [3] ○ Dietz and White [4] formulas 1 and 3 with $T_f = T_g$ —Janeschitz-Kriegl [3] formula 25 with Ω according to (11a) ($T_f = 180°C$) □ Janeschitz-Kriegl [3] formula 25 with Ω according to (11b) ($T_f = 180°C$)

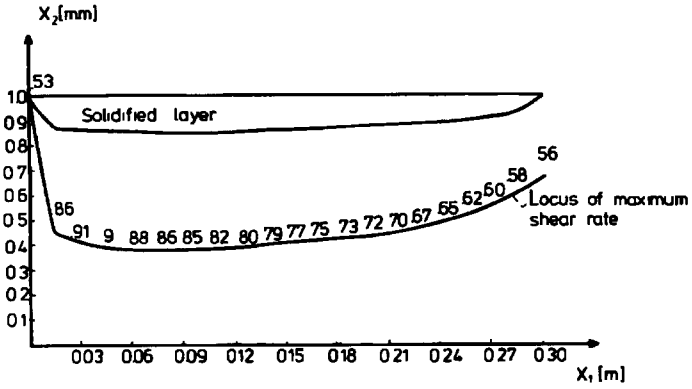

Fig 10 The locus of maximum shear rates for the moment that the mould has just been filled The numbers along the locus of maximum shear rate denote the value of the maximum shear rate in $10^3\ s^{-1}$

Janeschitz-Kriegl [3] (See Fig 9) The shape of the solidified layer according to Dietz and White is very different from the one found with the present theory This is probably due to the fact that Dietz and White use the isothermal velocity profile in the liquid phase, which is quite a rough approximation (Fig 11) The solidified layer found by the present authors is in moderate agreement with the one found by Janeschitz-Kriegl for $T_1 = 180°C$ This is quite remarkable since Janeschitz-Kriegl only discusses the heat transfer in and close to the solidified layer

Figure 10 shows the line on which the maximum value of the shear rate is reached The value of this maximum is a function of x_1 It is remarkable that

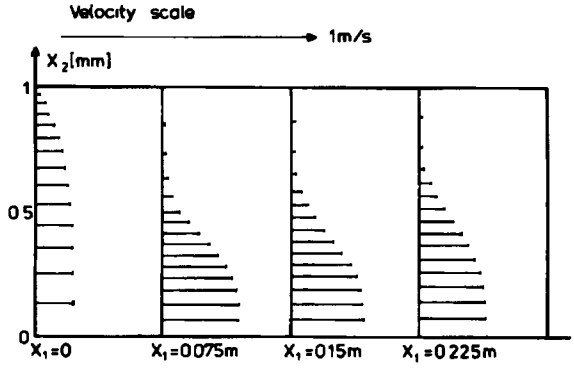

Fig 11 The velocity distribution at several positions for the moment that the mould has just been filled

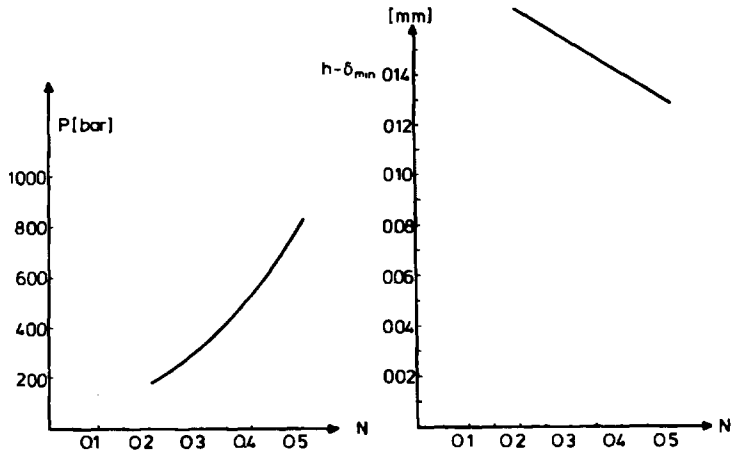

Fig 12 Influence of the value of n on the pressure drop and the maximum thickness of the solidified layer for the moment the mould has just been filled

this line lies so close to the axis of the mould This fact is emphasized by Fig 11, where the velocity distribution at several axial positions is given Due to the cooling action the molten polymer close to the solidified layers has a lower temperature than the core Since the viscosity decreases with increasing temperature, the fluid is forced to flow through the relatively hot region near the core

To obtain some insight into the dependence of the solution on variations

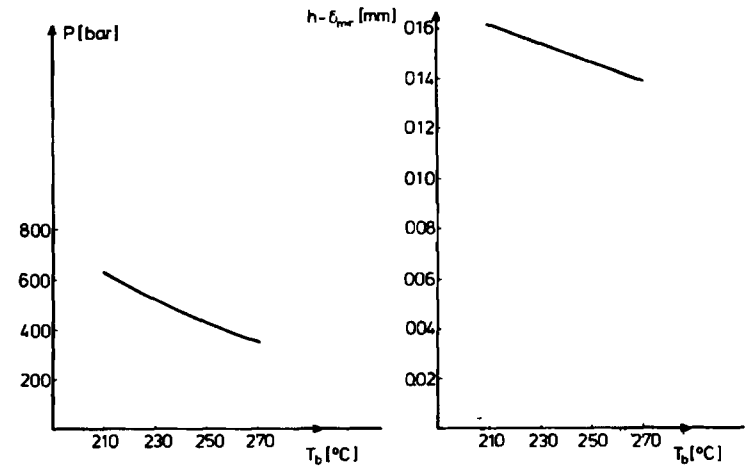

Fig 13 Influence of the injection temperature on the pressure drop and the maximum thickness of the solidified layer for the moment the mould has just been filled

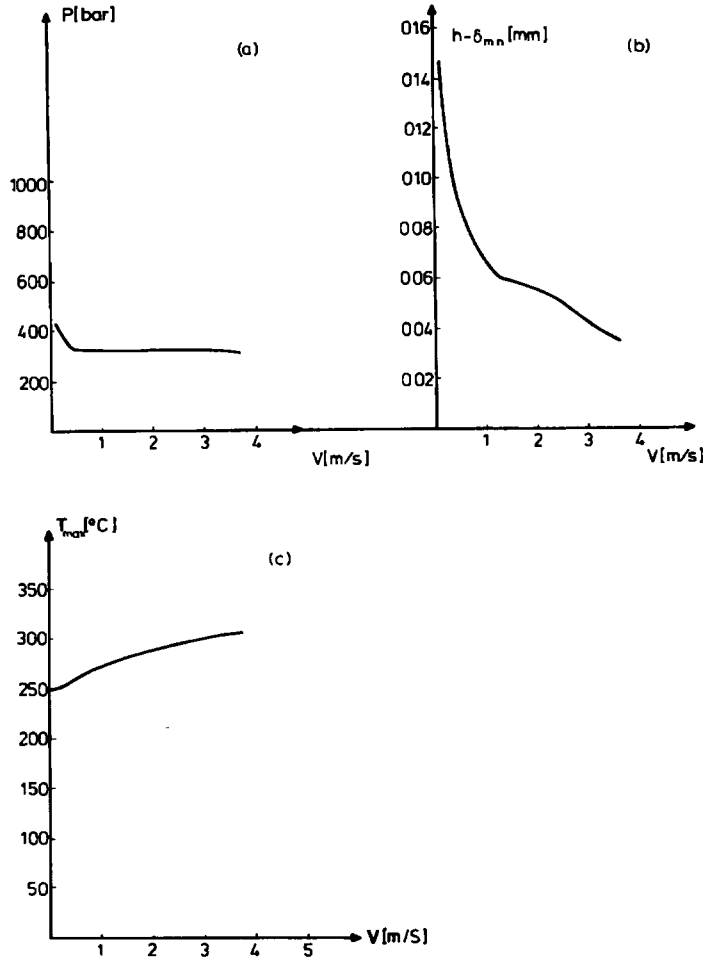

Fig 14 Influence of injection speed on the pressure drop the maximum value of the thickness of the solidified layer and the maximum temperature rise for the moment the mould has just been filled

of several input parameters, we carried out a series of numerical experiments Figure 12 shows the dependence of the total pressure drop and the maximum value of the thickness of the solidified layer on n at the moment the mould has just been filled

All other input data are equal to those for the case discussed at the beginning of this section We see that the pressure drop is extremely sensitive even to small variations of n This result emphasizes the need for accurate viscometric data of the polymer used in order to simulate the injection

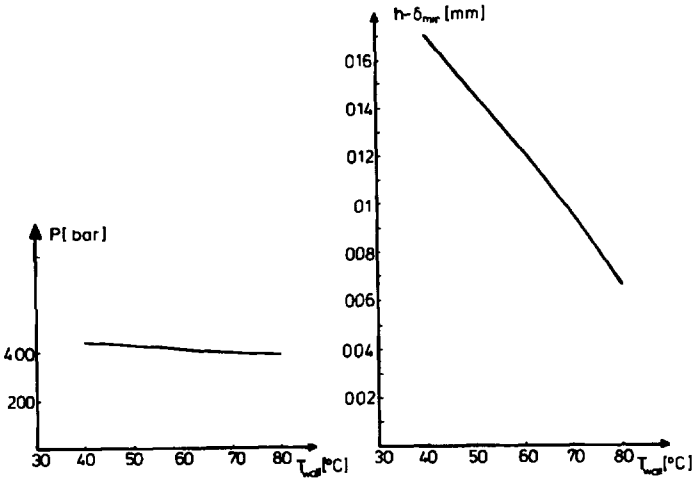

Fig 15 Influence of the wall temperature on the pressure drop and the maximum value of the solidified layer thickness for the moment the mould has just been filled

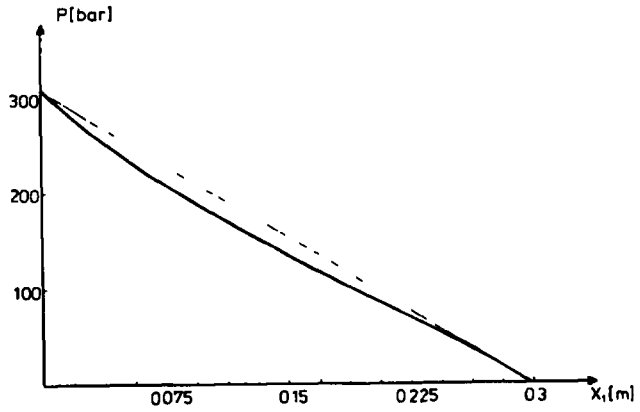

Fig 16 Pressure distribution for $v = 3.6$ m/s ($\beta = 0.7$)

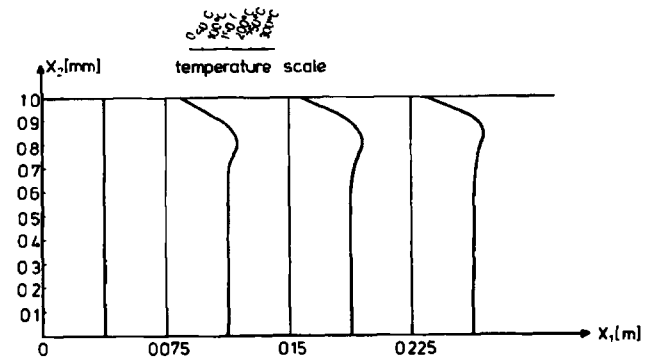

Fig 17 Temperature distribution at several positions for the moment the mould has just been filled $v = 3.6$ m/s ($\beta = 0.7$)

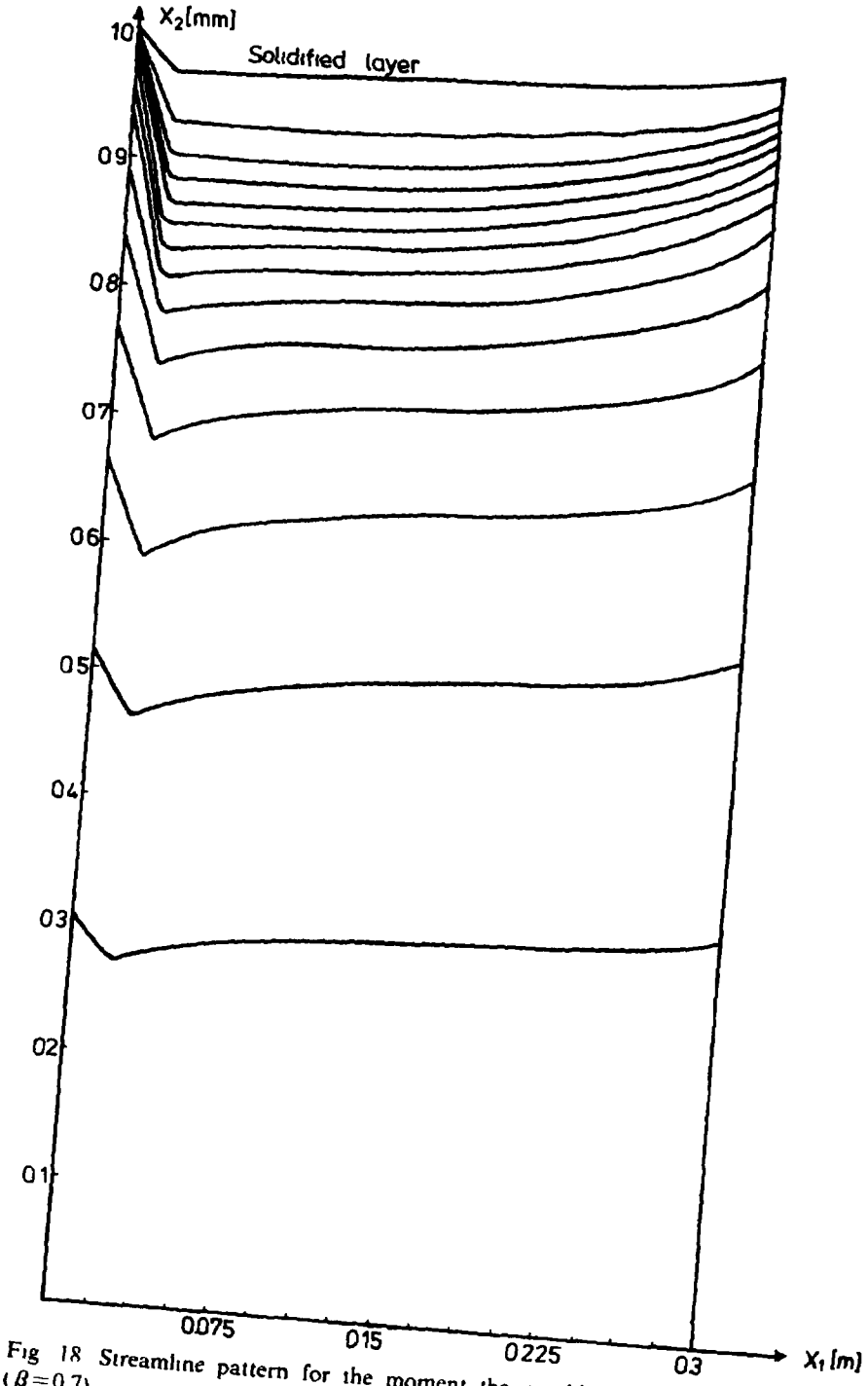

Fig 18 Streamline pattern for the moment the mould has just been filled ($t = 3.6$ m, $\beta = 0.7$)

moulding process properly The process parameters that can be changed are the injection temperature, the injection speed and the temperature of the walls

The results are presented in Figs 13, 14 and 15 It is surprising that above a certain injection speed the total pressure drop no longer changes The influence on the solidified layer thickness, however, is profound Obviously an equilibrium is reached between on the one hand the pressure-drop-increasing effect of the higher injection velocity and on the other hand the pressure-drop-decreasing effect of the lowering of the viscosity due to the higher shear rate and higher temperature The wider channel also decreases the pressure drop

The case $v = 3\,6$ m/s is worked out in more detail The characteristic numbers are

$Re = 0\,18$, $Bi = 7\,7 \times 10^{3}$ $Br = Na = 42$,
$Gz = 510$, $Ste = 25$,

where $\epsilon = 0\,01$, $\eta_0 = 21$ Pa s and $A = 0\,85$ In the channel approximation the number expressing the relative magnitude of the acceleration and the viscous terms in the equation of motion is equal to ϵRe Thus, in the case considered acceleration terms are still negligible

Figure 16 shows the pressure distribution along the axis of the mould The temperature distributions in several positions for the moment that the mould has just been filled are shown in Fig 17 Notice that due to the large amount of frictional heat the polymer is warmed up during injection The streamline pattern at the end of the filling stage is presented in Fig 18

References

1 J L S Wales, J van Leeuwen and R van der Vijgh, Polym Eng Sci, 12(5) (1972) 358–363
2 H Janeschitz-Kriegl, Rheol Acta, 16 (1977) 327–339
3 H Janeschitz-Kriegl, Rheol Acta 18 (1979) 693–701
4 W Dietz and J L White, Rheol Acta, 17 (1978) 676–692
5 W Dietz J L White and E S Clark Polym Eng Sci 18(4) 1978 273–281
6 H H Winter, Advances in Heat Transfer 1977 pp 205–268
7 J R A Pearson, J Fluid Mech, 83(1) (1977) 191–206
8 H Ockendon J Fluid Mech, 93(4) (1979) 747–746
9 H Ockendon and J R Ockendon, J Fluid Mech, 83(1) (1977) 177–190
10 R B Bird, A C Armstrong and O Hassager, Dynamics of polymeric liquids Wiley, New York, 1977, chapters 1 and 5
11 R B Bird, W E Stewart and E N Lightfoot, Transport Phenomena Wiley, New York 1960, chapter 9
12 F Neumann, Cf P Frank and R von Mises, Die Differential und Integral Gleichungen der Mechanik und Physik, Vol 2, Vieweg, Braunschweig, 1927

13 J L S Wales, The Application of Flow Birefringence to Rheological Studies of Polymer Melts, Delft University Press, 1976
14 Kenndaten fur die Verarbeitung thermoplastischer Kunststoffe Teil 1, Thermodynamik Carl Hanser Verlag, Munchen, Wien, 1979
15 Z Tadmor, J of Appl Polym Sci 18 (1974) 1753–1772